UDC 614.2, 614.8, 612.014.43, 551.582.3
DOI: 10.21668/health.risk/2025.2.04.eng

Read online

Research article

ASSESSING ECONOMIC LOSSES FROM RISKS OF HEAT-RELATED PREMATURE MORTALITY USING SATELLITE MAPPING IN RUSSIAN MEGACITIES

V.I. Gornyy[1], S.G. Kritsuk[1], I.Sh. Latypov[1], A.A. Tronin[1], R.V. Buzinov[2], S.N. Noskov[2], G.B. Yeremin[2], D.S. Borisova[2]

[1]Saint Petersburg Federal Research Center of the Russian Academy of Sciences, 39, 14th Line V.O., St. Petersburg, 199178, Russian Federation
[2]North-West Public Health Research Center, 4, 2nd Sovetskaya St., St. Petersburg, 191036, Russian Federation

This research aims to address the challenges associated with utilizing satellite imagery to create maps of economic losses due to premature deaths caused by urban heat stress in the Russian cities of Omsk and Rostov-on-Don.

The study intends to provide quantitative data that can be utilized for economic decision-making processes in the areas of environmental safety and public health. It suggests a theoretically substantiated satellite-based approach to map potential risks, mortality rates, and economic losses associated with heat-related fatalities. This approach has the potential to translate long-term satellite observations of urban temperatures into actionable recommendations for urban planning and health management strategies. The relevance of this research stems from the ongoing global concern regarding climate change and its negative impact on the health of urban residents.

Our research team has created digital maps of two significant cities, Omsk and Rostov-on-Don, each with similar populations but differing climatic conditions. These maps show the number of deaths associated with heat-related events as well as the associated economic losses. Their spatial resolution is 100 × 100 m, which allows analyzing a situation in a city as whole and within its municipal districts. Having compared the results obtained by satellite mapping with medical statistics per some Omsk districts, we have assessed the accuracy of our methodology to be approximately 20 %. Our findings emphasize both the advisability to make strategic investments in mitigating risks of urban environment overheating in areas with a high potential for increased mortality from heat-related causes and the potential value of utilizing this information in urban planning initiatives aimed at adapting healthcare systems to global warming.

Keywords: *climate warming, urban heat islands, megacities, Omsk, Rostov-on-Don, overheating, risk, heat-related mortality, satellite, mapping, economic losses.*

In the context of climate warming [1] there is a significant concern regarding safety of urban residents due to increased mortality rates associated with urban heat island effects and the occurrence of 'heat waves' able to considerably increased normal temperatures [2, 3]. These events can lead to significant economic costs due to ad-

Victor I. Gornyy – Candidate of Geological and Mineralogical Sciences, Head of the Laboratory of Remote Methods of Geoecological Monitoring and Geoinformatics (e-mail: v.i.gornyy@mail.ru; tel.: +7 (812) 499-64-54; ORCID: http://orcid.org/0000-0001-9706-6919).

Sergey G. Kritsuk – Senior Researcher of the Laboratory of Remote Methods of Geoecological Monitoring and Geoinformatics (e-mail: sit.bloom@gmail.com; tel.: +7 (812) 499-64-54; ORCID: https://orcid.org/0000-0002-3781-322X).

Iskander Sh. Latypov – Candidate of Physical and Mathematical Sciences, Senior Researcher of the Laboratory of Remote Methods of Geoecological Monitoring and Geoinformatics (e-mail: liscander@mail.ru; tel.: +7 (812) 499-64-54; ORCID: http://orcid.org/0000-0001-8653-7308).

Andrei A. Tronin – Doctor of Geological and Mineralogical Sciences, Director of the Scientific Research Center of Ecosafety of the Russian Academy of Sciences (e-mail: a.a.tronin@gmail.com; tel.: +7 (812) 499-64-54; ORCID: http://orcid.org/0000-0002-7852-8396).

Roman V. Buzinov – Doctor of Medical Sciences, director (e-mail: info@s-znc.ru; tel.: +7 (812) 655-62-26; ORCID: https://orcid.org/0000-0002-8624-6452).

Sergey N. Noskov – Candidate of Medical Sciences, Senior Researcher (e-mail: info@s-znc.ru; tel.: +7 (812) 655-62-26; ORCID: http://orcid.org//0000-0001-7971-4062).

Gennadiy B. Yeremin – Candidate of Medical Sciences, Head of the Department of Hygiene, Leading Researcher (e-mail: info@s-znc.ru; tel.: +7 (812) 655-62-26; ORCID: https://orcid.org/0000-0002-1629-5435).

Daria S. Borisova – Junior Researcher (e-mail: info@s-znc.ru; tel.: +7 (812) 655-62-26; ORCID: https://orcid.org/0000-0002-0694-5334).

ditional deaths attributed to climate-related factors, including rising average temperatures worldwide; these costs are estimated to be between $6 billion and $88 billion annually[1]. In recent decades, large cities in Russia have experienced an unprecedented increase in air temperature compared to surrounding rural areas. This phenomenon, known as the urban heat island effect, has been attributed to several factors. The urban heat island is a result of high levels of anthropogenic heat production, which is generated by such activities as industry, transportation, and residential use of energy. Additionally, reduction of cooling effects from evaporation due to lack of green space and sealing of soil by road pavement contributes to the increased temperatures. Other factors that contribute to the urban heat island include concentrations of greenhouse gases and intensive heating of metal roofs by solar radiation, which have low thermal inertia. These factors lead to overheating of urban areas relative to rural areas. An optimal air temperature has been established to exist for each location, within which the lowest mortality rate is observed[2] [4–6]. As the average daily air temperature exceeds the threshold temperature for the lowest mortality, the annual death toll also increases. This conclusion is based on statistically supported epidemiological studies that have demonstrated a correlation between the relative risk of mortality and the average daily air temperature [4, 5, 7].

In light of climate change, an international team of scientists, based on a study of temperature trends between 1984 and 2015, has made several long-term forecasts regarding the estimated levels of additional deaths in various countries worldwide. The study reveals a negative outlook for all countries and calls for development of effective measures to protect and adapt populations to rising temperatures [8]. This requires development of efficient methods for monitoring heat-related mortality (HRM) in order to adapt public strategies accordingly. Extreme heat periods have a more significant impact on mortality from cerebrovascular diseases than from ischemic heart diseases [9]. Furthermore, prolonged hot weather leads to an increase in mortality from cardiovascular diseases, particularly among older individuals [10]. According to a meta-analysis of studies, ambient air temperature and its fluctuations have various implications for development of meteopathic reactions. A large-scale study conducted between 2004 and 2008 in the United States analyzed 7,758 cases and found that it was not possible to definitively determine impacts of seasonal variations in temperature, humidity, and atmospheric pressure on health. However, other studies have found correlations between atmospheric temperature and various health conditions. For example, a study [11] found a direct link between air temperature and prevalence of ischemic strokes. They identified a negative correlation between air humidity and stroke incidence and also found a correlation between increased emergency medical calls for circulatory diseases such as cardiac arrhythmia, arterial hypertension, and heart failure and higher air temperatures. It has also been observed that t_m (lowest mortality temperature) is influenced by climate. For individuals residing in southern latitudes, t_m is generally higher than for those in more northerly regions[1] [12, 13]. Even within a single city, there may be significant variations in average daily air tem-

[1] MR 2.1.10.0033-11. Otsenka riska, svyazannogo s vozdeistviem faktorov obraza zhizni na zdorov'e naseleniya: Metodicheskie rekomendatsii, utv. Rukovoditelem Federal'noi sluzhby po nadzoru v sfere zashchity prav potrebitelei i blagopoluchiya cheloveka, Glavnym gosudarstvennym sanitarnym vrachom Rossiiskoi Federatsii G.G. Onishchenko 31 iyulya 2011 g. [The Methodical Guidelines 2.1.10.0033-11. Assessment of health risks associated with impacts exerted on health by lifestyle-related factors: Methodical guidelines, approved by G.G. Onishchenko, Head of the Federal Service for Surveillance over Consumer Rights Protection and Human Wellbeing, the RF Chief Sanitary Inspector on July 31, 2011]. *KODEKS: electronic fund for legal and reference documentation*. Available at: https://docs.cntd.ru/document/1200111974?ysclid=mbows1mjec956425907 (November 12, 2024) (in Russian).

[2] ISO 7730:2005. Ergonomics of the thermal environment – Analytical determination and interpretation of thermal comfort using calculation of the PMV and PPD indices and local thermal comfort criteria: International Standard, 3rd ed., 52 p.

peratures[3] [14–16]. Furthermore, *t* may differ by several degrees within different parts of a city. This can lead to an uneven distribution of mortality rates due to heat stress in various parts of the urban environment [16, 17]. In order for city authorities to make informed decisions regarding management of threats to population health posed by urban overheating, it is essential to have detailed information on spatial distribution of the average economic impact caused by premature deaths resulting from overheating. Bearing in mind that management decisions should be based on averaged long-term data, estimates should rely on a long-term analysis of time-series data obtained for each pixel in a map. From an economic standpoint, it is advantageous to utilize archival satellite data, as its analysis yields a map of the land surface temperature on the survey day. However, this approach has a drawback, as it may be difficult to obtain continuous time-series data due to cloud cover. This can prevent creation of a statistically representative distribution of averaged daily temperatures. Several methods could be employed to address this limitation. For example, at the time of data collection, an air temperature map is generated using the multiple correlation technique based on satellite imagery in combination with ground-based measurements of various characteristics of the urban environment. These measurements include, among others, the vegetation index and the height of surface relief. The distances from the coastline are also recorded [18–22]. A disadvantage of this approach is difficulty in generating a statistically significant number of maps needed to estimate a specific risk of overheating events.

Recent research has focused on developing methods to generate maps of deaths due to overheating on a specific date. For this purpose, maps of brightness temperatures acquired by thermal surveys conducted by Terra/Aqua(MODIS) satellites, ground-based measurements, and other characteristics of the urban environment were used, as well as statistical data on the number of urban deaths that occurred at various air temperatures [18–20]. This methodological approach to creating a digital map of mortality rates has some limitations. In order to make management decisions, we require more detailed spatial information than can be obtained from a grid with a resolution of 1×1 *km*. Moreover, this digital map is created at a particular point in time, so it is not possible to generate a statistically significant number of digital maps over a long period, and consequently, it is not possible to average potential data over a long time. In addition, collecting a large number of meteorological observations over several years using a representative ground-based observational network extends the timeframe for obtaining results.

Mathematical modeling of a large number of temperature measurements is possible but it would require significant computational resources and long-term validation of the model.

Recently, a new method for satellite-based mapping of air temperature has been developed [15]. This method combines the results of periodic satellite thermal surveys (spatial data), which were accomplished in cloudless periods, with long-term continuous air temperature monitoring data from standard weather stations (time-series data). This allows for the mapping of risk of population mortality and potential economic damage resulting from urban overheating [16]. Further development of this technique has led to the creation of mathematical expectation of economic losses due to premature heat-related mortality (HRM) caused by overheating events in urban areas [17]. As a result, based on the case study of Helsinki (Finland), it has been demonstrated that there is a spatial heterogeneity of heat-related economic losses that necessitates a differentiated approach to measures designed to mitigate the threats to public health posed by climate change. This technique has the potential to be used as a tool for forecasting and

[3] Bornstein R.D. Observations of the Urban Heat Island Effect in New York City. *Journal of Applied Meteorology*, 1968, vol. 7, no. 4, pp. 575–582.

mitigating economic damage associated with urban overheating in future. However, at present it is rather difficult to implement it in practice since it is very labor-intensive. Therefore, in this study, we **aim** to develop a simplified approach for satellite-assisted HRM mapping in two megacities located in various climatic regions and to explore the commonalities in the spatial occurrence of premature HRM incidents.

Theoretical grounds, materials and methods. The main principle behind our initial attempt to create maps of mortality rates and economic losses due to premature heat-related mortality (HRM) is to identify correlations between *T(x, y)* – the land surface brightness temperatures at each *(x, y)* – element of a given territory (corresponding to a pixel in a map) and *t(τ)* – urgent air temperatures recorded at weather stations over time. This approach, which combines spatial data from satellites with time-series data from weather stations, has been validated using available mortality data from Helsinki [16, 17]. However, it has also been identified as an extremely labor-intensive process, so in this study we have sought to develop a more streamlined methodology for analyzing aggregated data.

Epidemiological studies have demonstrated that in cities where *t* is an average daily air temperatures increase, the rate of mortality also increases in the entire population. The mortality rate, *‰/day* per day is calculated as $\mu_M(t) = M_M(t)/(N \cdot 10^{-3})$ the number of daily deaths due to all causes (*deaths/day*) divided by the number of residents in the city (*N*). The dependence of $\mu_M(t)$ on t – daily average air temperature can be represented by a second-order algebraic function. The annual mortality rate, $\overline{\mu}_M$, is defined as the annual number of deaths per 1000 residents.

Approximation of medical statistics data (Figure 1) suggests that when $t \geq t_m$, (where t_m – the temperature of minimum mortality, ^oC) the temperature dependence of $\mu_M^+(t)$ – the daily mortality rate due to overheating in a city, *‰/day* (where the subscript «*M*» denotes medical statistics), can be represented by a quadratic function:

$$\mu_M^+(t) = \mu_M(t) - \mu_M(t_m) = \\ = \gamma \cdot (t - t_m)^2, \quad t > t_m, \tag{1}$$

where $\mu_M(t_m)$ is all-cause mortality rate, ‰/day at t_m. It is possible to assume that over the 20-year period of repeated satellite surveys, the mortality rate for a particular city has remained consistent. γ is a coefficient.

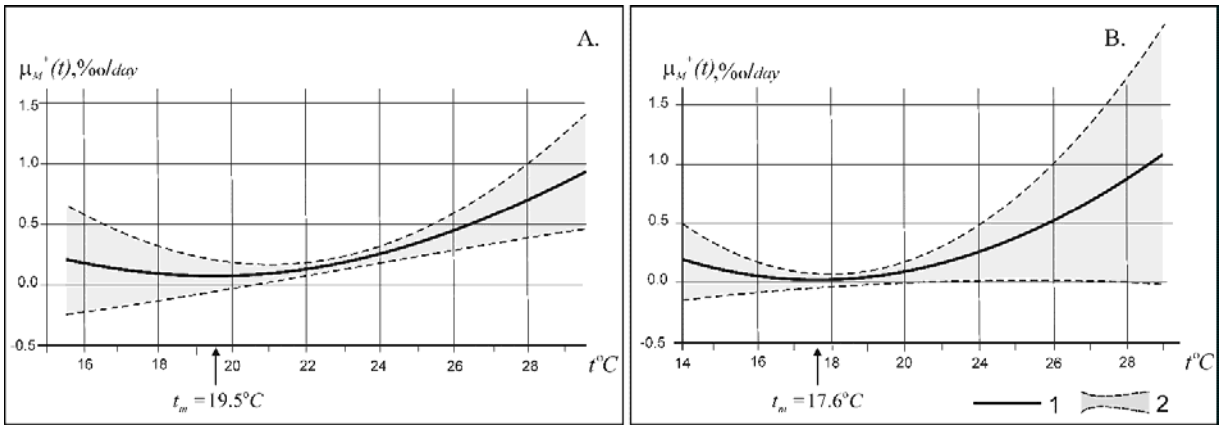

Figure 1. Approximation of dependence $\overline{\mu}_S^+(i)$ on *t*: A. Rostov-on-Don: $\mu_M^+(t) = 0.012t^2 - 0.4225t + 3.7482$; B. Omsk: $\mu_M^+(t) = 0.0082t^2 - 0.3255t + 3.2359$ (Legend: 1. Approximation. 2. Confidence intervals of approximation with a probability of 90 %)

In the context of the approximate equation (1), the task of satellite-based mapping of mortality rates can be reduced to the compilation of $\overline{\mu}_S^+(x,y)$ – maps of statistically averaged (potential) annual specific mortality rates due to overheating, based on satellite data for the (x, y) area of a pixel, $‰ / (km^2 \cdot year)$. In other words, it is necessary to spatially distribute $\overline{\mu}_M^+$ – the annual mortality rates, *‰/year* due to heat exposure across the city.

The search for a solution to this issue is hampered by the fact that information on daily average air temperature is available only at weather stations. The only data that can be utilized to determine the mortality rate in a city is $T(x,y,i)$ – the brightness temperature, *K*, of the land surface, which is derived from Landsat satellite data at coordinates $x = 1,...,X; y = 1,...,Y$. This data is accessible at each point within the city. Based on this information, we can assume that $\overline{\mu}_M^+(x,y)$ – the specific mortality rate due to overheating in a pixel area with coordinates $x = 1,\ldots,X; y = 1,\ldots,Y,$ on a given *i*-th day can be approximated as:

$$\overline{\mu}_M^+(x,y,i) = \beta \cdot \left[n(x,y) \cdot T(x,y,i) - T_* \right]^2, \quad (2)$$

where β_i is a coefficient;

$n(x,y)$ is population density, residents (x, y) in a pixel, residents/km^2, which, similar to surface temperature, influences mortality;

T_* is a brightness temperature of the underlying surface (analogous t_m), K.

Next, we sum (2) over all the coordinates, which allows us to use the mortality data obtained from medical statistics:

$$\mu_M^+(i) = \beta \cdot S(i), \quad (3)$$

where $S(i) = \sum_{x=1;\, y=1}^{X,Y} n(x,y) \cdot \left[T(x,y,i) - T_* \right]^2$,

and T_* is a constant, determined on the base of analyses of satellite data (see Figures 2 and 3).

Let's assume that β does not depend on time. That is, $\mu_M^+(i)$ only depends on meteorological conditions on a day an image was made. To do this, we will develop a regression model of $\mu_M^+(i)$ based on all available data points for all *i*.

The parameter T_* is selected by minimizing the ratio of the standard deviation of β – the slope to its mean value (Figure 2), which corresponds to the maximum value of R^2 for the regression equation (Figure 3).

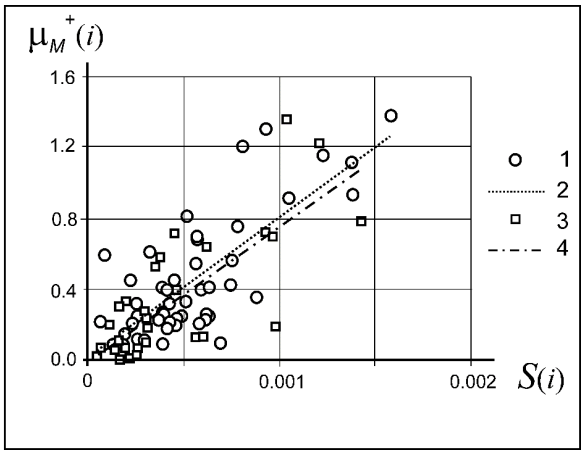

Figure 2. The dependence of $\mu_M^+(i)$ on $S(i)$. The value of T_* is shown to be optimal, providing the maximum value of R^2 (see fig. 3) (Legend: Rostov-on-Don: 1. $\overline{\mu}_M(i)$; 2. Regression for the all Landsat surveys, $i = 1,\ldots, I$; Omsk: 3. $\overline{\mu}_M(i)$; 4. Regression for the all Landsat surveys, $i = 1,\ldots, I$)

Therefore, the coefficient β is determined from the regression (Figure 2).

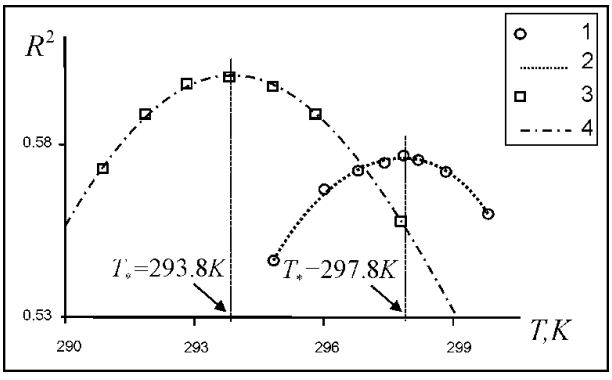

Figure 3. T_* – parameter selection (Legend: Rostov-on-Don – 1. $\overline{\mu}_M(i)$; 2. Regression for $i = 1,\ldots, I$; Omsk – 3. $\overline{\mu}_M(i)$; 4. Regression for $i = 1,\ldots, I$)

Next, $\hat{\mu}_M^+$ is the mortality rate, *‰/day:* due to heat stress, according to medical statistics, averaged over all surveys:

$$\hat{\mu}_M^+ = \left[\sum_{i=1}^{K} \mu_M^+(i) \right] / K. \quad (4)$$

After that, $\hat{\mu}_S^+(x,y)$ is the specific mortality rate from overheating at (*x, y*) – an elementary site averaged over all days when the satellite imagery was carried out, ‰/day was calculated for each satellite survey day based on $T(x,y)$ – the land surface brightness temperature of the area corresponding to the pixel (*x, y*):

$$\hat{\mu}_S^+(x,y) = \\ = \{\beta \cdot \sum_{i=1}^{K} n(x,y) \cdot [T(x,y,i) - T_*]^2\} / K. \quad (5)$$

The proportion of the mortality rate $\varphi(x,y)$ for a specific area, which corresponds to the pixel (*x, y*) in the total mortality rate of the city, can be calculated as:

$$\varphi(x,y) = \hat{\mu}_S^+(x,y) / \hat{\mu}_M^+ . \quad (6)$$

Therefore, the annual specific mortality rate due to overheating in the pixel area (*x, y*):

$$\bar{\mu}_S^+(x,y) = \varphi(x,y) \cdot \bar{\mu}_M^+ , \quad (7)$$

where $\bar{\mu}_S^+(x,y)$ and $\bar{\mu}_M^+$, $‰ / (year \cdot km^2)$ are the potential mortality rates resulting from overheating, which were obtained, respectively, through satellite imaging and medical statistics.

After that, $\bar{M}_S^+(x,y)$ or the specific annual number of deaths within the pixel's territory (*x,y*), $deaths / (year \cdot km^2)$, can be written as:

$$\bar{M}_S^+(x,y) = \bar{\mu}_S^+(x,y) \cdot n(x,y) \cdot 10^{-3}, \quad (8)$$

where *n*(*x, y*) is the number of individuals in the elementary unit (*x, y*). Hence, $\bar{M}_S^+$ is the annual number of deaths, *deaths/year,* from overheating per year in area A, km^2 according to satellite data:

$$\bar{M}_S^+(A) = \sum_{x,y}^{A} \bar{M}_S^+(x,y). \quad (9)$$

When analyzing the results, it is beneficial to have a representation of $r(x,y)$ as the risk (probability) of air temperature exceeding a threshold t_m. To achieve this, we employ a previously developed methodology [16] that involves identifying, for each individual pixel, the correlation between *T(x, y)* and *t* at designated weather station:

$$r(x,y) = \sum_{j \to t_m}^{i=J} p_j \left[t_{eq}(x,y) \right], \quad (10)$$

where $p_j \left[t_{eq}(x,y) \right]$ is the frequency distribution of the equivalent temperature within *j*-th each bin of the histogram, with *j* = 1,..., *J*; $t_{eq}(x,y)$ is the equivalent temperature. This is the average daily air temperature, recorded at the weather station that corresponds to *T(x, y, i)*, the brightness temperature measured at the time of a satellite survey carried out on the *i*-th day.

The temperature interval of the histogram is 1 °C for the weather station, starting from t_{eq} = 0 °C and up to $t_{\max}$ as the maximum daily average air temperature historically recorded by the weather station. Due to this linear dependence, we can derive a regression equation:

$$t = t_{eq}(x,y,i) = a \cdot T(x,y,i) + b. \quad (11)$$

Given this linear relationship, it is possible to linearly transform the statistical distribution:

$$p_j \left[t_{eq}(x,y) \right] = a(x,y) \cdot p_j(t) + b(x,y).$$

Based on (9), calculation of $l(x,y)$, specific economic damage due to premature heat-related mortality, *$/(km² · year)* takes into account ε – the cost of a single premature HRM, $\$ / death$ and is given as (12):

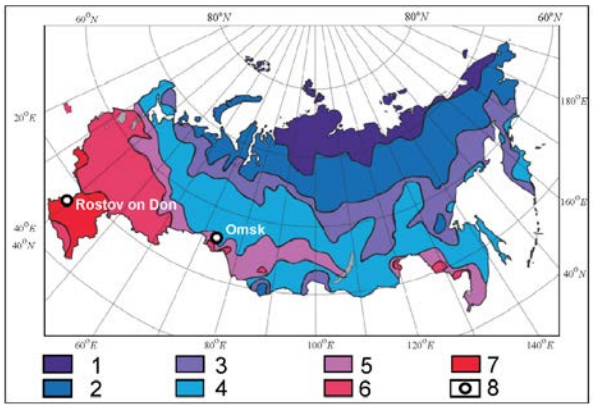

Figure 4. The map of the zoning of the Russian territory based on living conditions in the population [6]. Period: 2001–2010 (The legend: 1. Absolutely unfavorable zone; 2. Very unfavorable zone; 3. Unfavorable zone; 4. Conditionally unfavorable zone; 5. Conditionally favorable zone; 6. Favorable zone; 7. Most favorable zone)

$$l(x,y) = \varepsilon \cdot \bar{M}_S^+(x,y). \qquad (12)$$

Finally, $L(A)$ is the total average annual economic damage (potential economic damage) in locality or its district due to premature mortality, caused by heat stress, *$/year*:

$$L(A) = \varepsilon \cdot \bar{M}_S^+(A). \qquad (13)$$

Research objects. To develop a streamlined methodology for satellite-based mapping of economic losses due to HRM, two megacities with distinct living conditions and situated in various climatic zones of Russia were chosen: Rostov-on-Don and Omsk. Figure 4 provides a visual representation of the selected cities per living conditions. Table 1 presents basic information necessary for understanding the medical and climatic situation in these cities.

For satellite mapping of economic damages from premature HRM, data from summer surveys by Landsat series satellites was used (Table 2). The temperature sensitivity of the Landsat 7 satellite was no worse than 0.3 *K*, and the initial spatial resolution was 60 meters (converted to 30 meters during processing)[4] [24]. The temperature sensitivity for the Landsat 8 satellite is 0.4 *K* at a background temperature of 300 *K* with a spatial resolution of 100 *m*. In addition, we used urgent summer air temperature observations at meteorological stations in the World Meteorological Organization (WMO) network for the entire period during which satellite data (Table 2).

Table 1

City profiles

No.	Name	Population, people	City area / area of green spaces, km^2	Latitude, degrees	Average air temperature in July, °C
1	Rostov-on-Don	1,142,000	348 / 77	47°14’ N	24.0
2	Omsk	1,126,000	578 / 130	54°56’ N	19.6

Table 2

Satellite materials and meteorological data used for mapping

№	City	Satellite	Number of scenes	Period, dd.mm.yyyy	Data source	WMO weather station code
1	Rostov-on-Don	Landsat 7 Landsat 8	37 26	31.07.2000– 30.08.2022	https://earthexplorer.usgs.gov	34730
2	Omsk	Landsat 7 Landsat 8	10 34	01.06.2013– 25.08.2022	https://earthexplorer.usgs.gov	28698

[4] Landsat 7 (L7) Data Users Handbook. Version 2.0. South Dakota, Sioux Falls, EROS Publ., 2019, 139 p.

To analyze the results of the study, we used maps of functional zones[5].

Data on population density in these cities were taken from the digital World population density maps, created by the European Union[6]. In addition, we used data on economic losses from one premature HRM event in each of the studied cities. For Rostov-on-Don, the estimated loss was $14,400 per death, and in Omsk it was $15,599 per death [23].

Baseline data on daily mortality in selected cities were provided by the Institute for Economic Forecasting at the Russian Academy of Sciences and the Federal Service for Surveillance over Consumer Rights protection and Human Wellbeing.

Figure 5 demonstrates the method for mapping the risk of overheating and potential HRM using the results from multiple satellite surveys. This method is built on the fundamental principles discussed above.

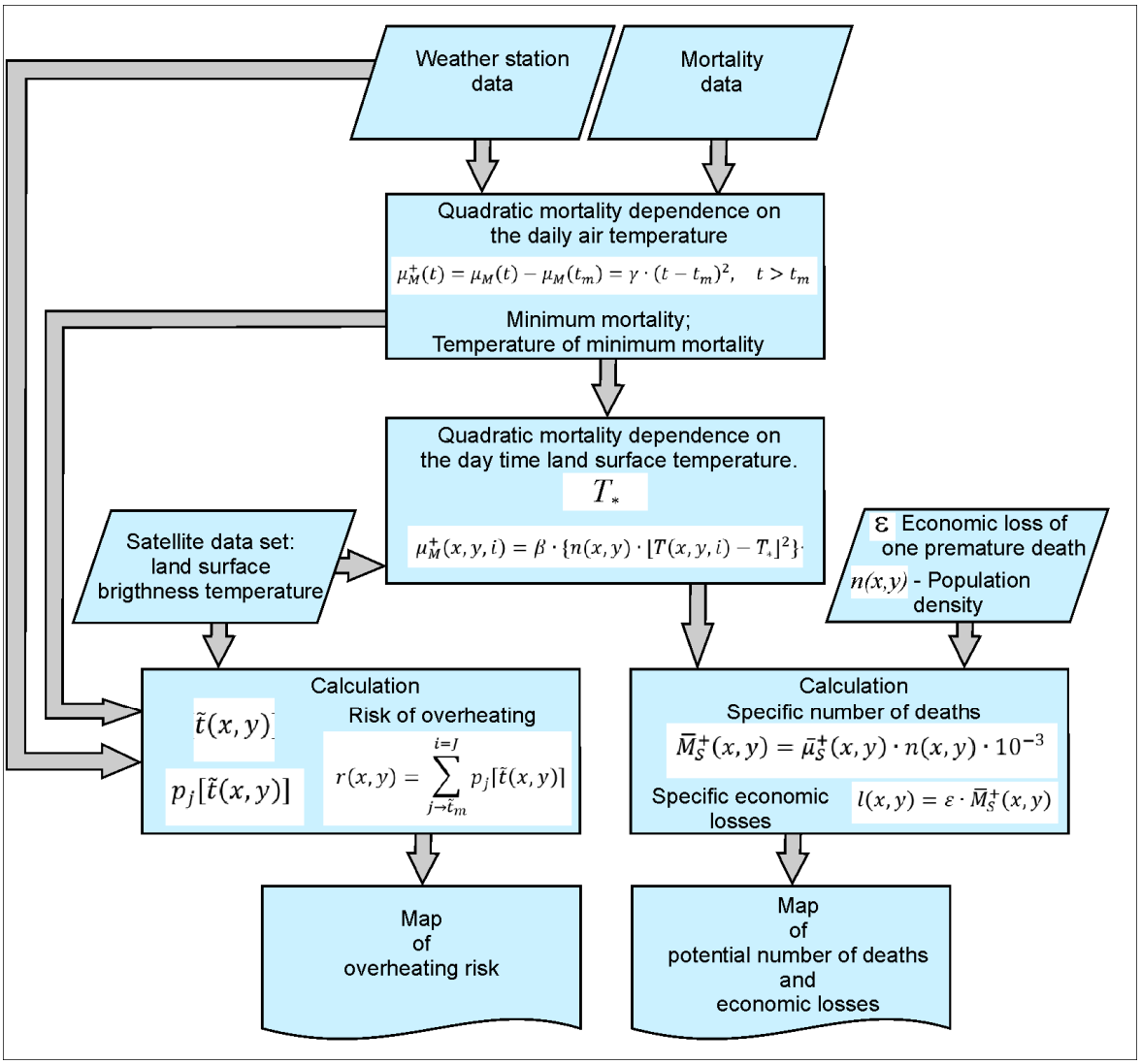

Figure 5. Information flow diagram for satellite mapping of risk of overheating and potential HRM

[5] Omsk. *World Population Density*. Available at: https://luminocity3d.org/WorldPopDen/#10/51.0280/34.8335 (November 16, 2024); General'nyi plan Rostova-na-Donu [The general Development Plan for Rostov-on-Don]. *Rostov-on-Don: City Duma and City Administration: official portal*. Available at: https://rostov-gorod.ru/administration/structure/departments/daig/action/01-grado-01-genplan/ (November 16, 2024) (in Russian).

[6] World Population Density. Available at: https://luminocity3d.org/WorldPopDen/ (November 16, 2024).

Results and discussion. The refined methodology for satellite-based mapping of risks and economic impacts due to HRM was tested using the cities of Omsk and Rostov-on-Don as case studies. Detailed maps were created showing the risk of air temperature exceeding the threshold for minimum mortality (Figures 6c and 7c).

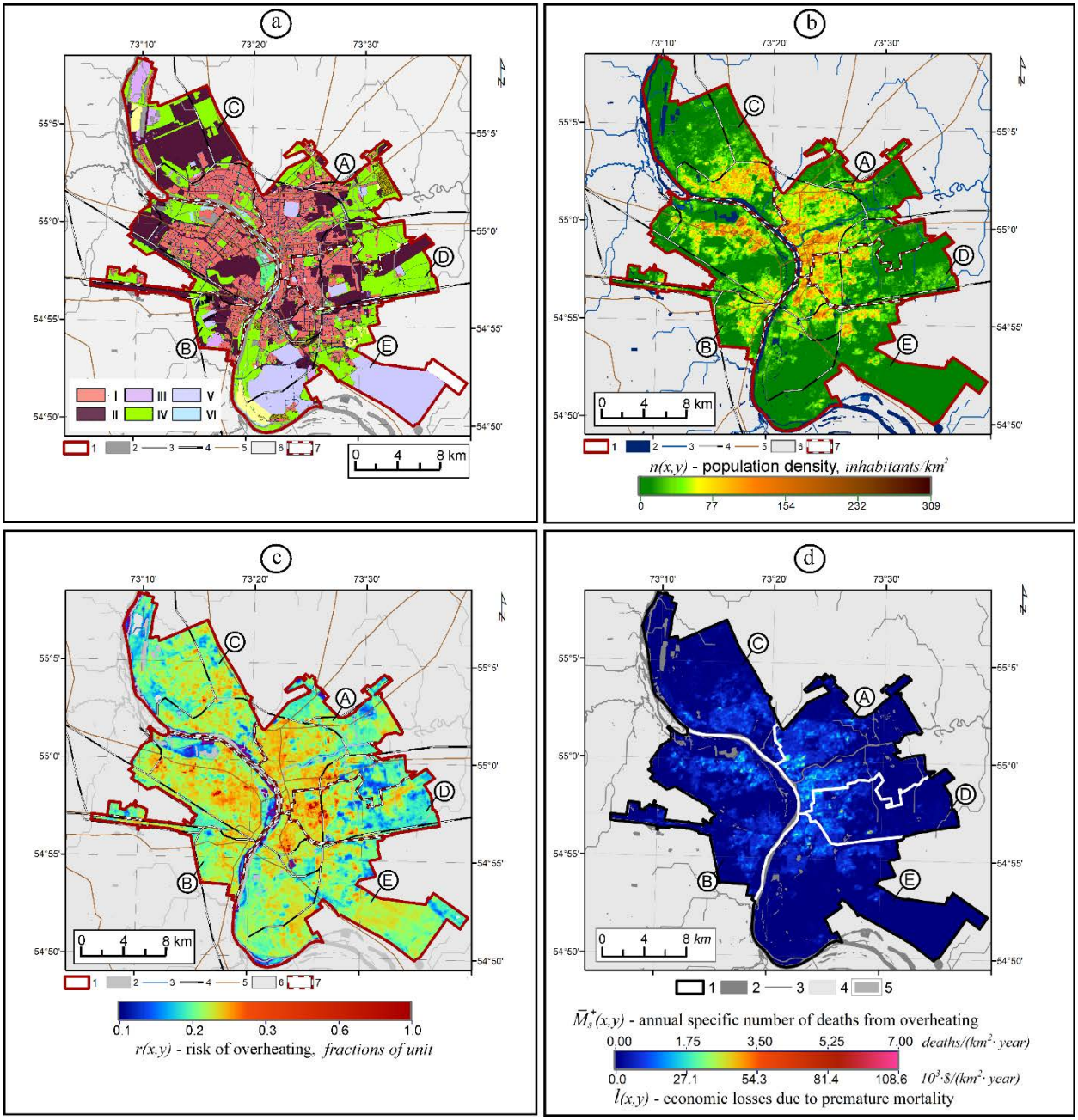

Figure 6. Satellite maps of city of Omsk (Russia) (Legend below maps: 1. City border. 2. Water areas. 3. Rivers. 4. Railways. 5. Car roads. 6. Suburb. 7. Borders of municipal districts. Capital letters in circles indicate municipal districts: A – Central. B – Kirovskiy. C – Sovetskiy. D – Oktyabrskiy. E – Leninskiy): (a) Simplified scheme of functional zones (Legend inside map: I. Buildings: residential low-rise, high-rise, public business, multifunctional, historical. II. Industrial and transport infrastructure. III. Waste storage and disposal. IV. Landscaped recreational, horticultural, cemeteries. V. Restricted territories. VI. Ponds); (b) Digital population density map (Period: 2020); (c) Digital map of $r(x,y)$ – risk of overheating; (d) Digital map of $\bar{M}_S^+(x,y)$ – specific number of deaths due to overheating and $l(x,y)$ – economic losses due to premature mortality caused by overheating

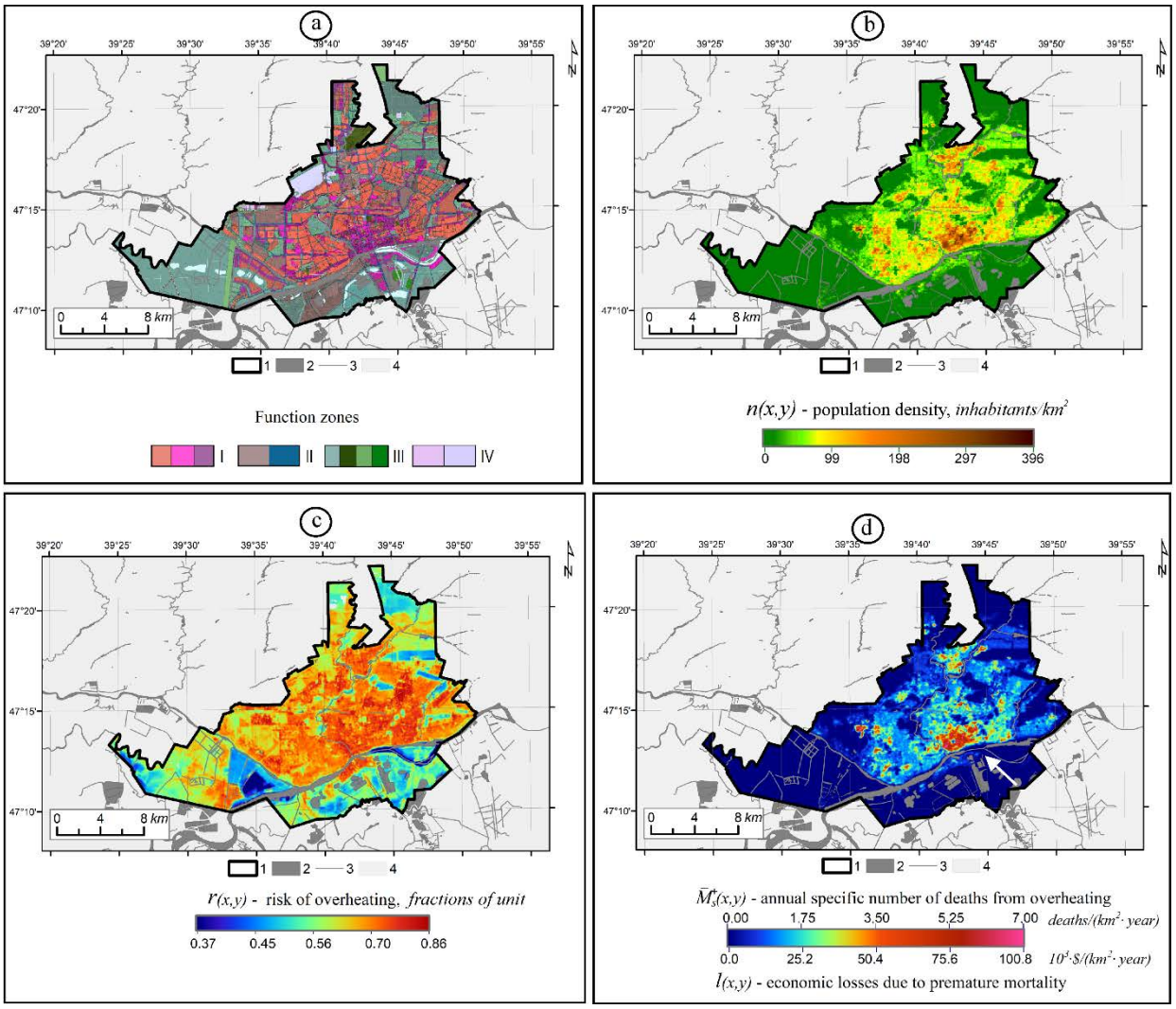

Figure 7. Satellite maps of city of Rostov-on-Don (Legend below maps: 1. City border. 2. Water areas. 3. Rivers. 4. Railways. 5. Car roads. 6. Suburb. 7. Borders of municipal districts): (a) Simplified scheme of functional zones (Legend below map inside Fig. (a): I. Buildings: residential low-rise, high-rise, public business, multifunctional, historical. II. Industrial and transport infrastructure. III. Landscaped recreational, horticultural, cemeteries. VI. Waste storage and disposal); (b) Map of $n(x, y)$ (Period: 2020); (c) Digital map of $r(x, y)$; (d) Digital map of $\bar{M}_S^+(x, y)$ and $l(x, y)$. The white arrow indicates an area with a high HRM

Table 3

Errors in Satellite Mapping of HRM in Omsk

Omsk municipal districts			Annual number of deaths due to HRM, deaths/year		Relative error of satellite technique, %
Letter designation in Fig. 6	Names of municipal districts	Population, people	Medicine statistics	Satellite mapping	
A	Central	245,578	17	20	+17
B	Kirovskii	248,209	19	16	-15
C	Sovetskii	204,001	11	10	-9
D	Oktyabrskii	271,440	14	8	-42
E	Leninskii	156,467	11	10	-9
Total City:		1,126,000	72	64	-11

Theoretical studies were validated using Omsk as an example, as statistical data on mortality were available not only for the entire city but also for its individual districts. This allowed us to assess the relative errors of our method for different districts of the city (see Table 3).

It is worth noting that in areas such as Sovetskii, Kirovskii, and Leninskii districts in Omsk, the relative errors did not exceed 15 %. This indicates a satisfactory result, given that these areas have a lower population density. In contrast, areas with a higher population density, such as Central (A at Fig. 6) and Oktyabrsky (D at Fig. 6), had relative errors ranging from 17 to 42 %. These initial results suggest that the relative error in the mapping of mortality and economic losses remains within 20 %, which is generally acceptable for economic assessments. An analysis of all satellite maps reveals that risks of heat stress, potential fatalities, and economic damage are not uniformly distributed within the studied cities. Increased potential mortality rates are concentrated in areas where high population density coincides with a higher risk of heat stress. This pattern is the most evident in urban centers such as the historical districts of Omsk and the core of Rostov-on-Don. Conversely, minimal mortality has been observed in areas with a high heat stress risk but low population density, for instance, in the Leninskii district of Omsk within areas for waste storage and disposal where there are no permanent inhabitants and therefore no heat-related mortality. It should be noted that obtaining more accurate mortality data presents a challenge due to difficulty in considering residents who may be present at workplaces that have different temperature conditions from their place of residence. In order to improve this technology, it may therefore be necessary to take into account daily patterns of population migration.

Satellite maps of mortality rates when compared with data collected through medical statistics reveal notable differences of approximately 10 % in Omsk and 4 % in Rostov-on-Don (see Table 4). These disparities are attributable to errors resulting from the statistical averaging process employed in the algorithm.

Comparison of Figures 4, 6, and 7 reveals an interesting result. Omsk is located on the border between the Conditionally Favorable and Conditionally Unfavorable zones, while Rostov-on-Don is situated within the Most Favored Zone. At the same time, HRM is higher in Rostov-on-Don compared to Omsk (see, Table 4 and Figures 6 and 7). This phenomenon can be explained by the fact that the Russian territory zoning map (Figure 4) was created based on an average of several zonal indicators, which were subsequently adjusted by azonal factors. The temperature indicator was only one of many factors, and therefore it was not the decisive factor in determining the zoning.

Further development of this technology may involve use of other relevant urban parameters. It is a known fact that over recent decades, the global temperature has grown leading to an increase in precipitation rates over land. With increased precipitation and temperature, absolute humidity levels of air

Table 4

Comparison of the main characteristics of annual HRM in the populations of Omsk and Rostov-on-Don

Annual characteristics	Omsk	Rostov-on-Don
Number of deaths according to medical statistics, deaths/year	72	152
The potential annual number of deaths due to satellite maps, deaths/year	64	146
HRM rate according to medical statistics, ‰/year	0.063	0.133
Potential HRM rate according to satellite maps, ‰/year	0.057	0.123
Economic losses from HRM according to medical statistics: Total city, $/year: Specific average: $/(year·km^2)	 $1.10 \cdot 10^6$ 1,903	 $2.19 \cdot 10^6$ 6,293
Potential economic losses from HRM according to satellite maps, $/year	$0.99 \cdot 10^6$	$2.10 \cdot 10^6$

are likely to increase as well. This could have implications for healthcare since higher air humidity levels with high temperature may cause the mortality rising.

The practical significance of detailed mapping of economic losses from HRM is illustrated by the following example. Mitigating urban HRM under climate change could be achieved through implementation of various technological solutions such as creation of green spaces, use of reflective surfaces, and installation of 'cold' metal roofs. For instance, costs of converting conventional roofs to 'cold' roofs ranges between $60 and $150 per square meter at present [25]. Therefore, if one square kilometer of conventional rooftops were replaced with 'cold' ones, it would cost between $60 million and $150 million. This is a significant amount that exceeds estimated annual economic losses due to HRM in Rostov-on-Don, which stands at $2.19 million. Given that the lifespan of a typical roof is approximately 30 years, the total cost of implementing sustainable roofing solutions over a 30-year period would be comparable to that of the economic impact of 'cold' rooftop installations in Rostov on Don. It is worth noting that implementation of 'cold' roofs may also contribute to reducing heating and climate control system costs [25]. As cities strive to address health risks posed by climate change, it is advisable to invest in measures that minimize urban heat island effects, particularly in areas with higher mortality rates. In the case of Rostov-on-Don, this encompasses the central district indicated by the arrow in Figure 7d, covering approximately 8 square kilometers of the city (out of a total area of 350 square kilometers). Satellite maps of potential economic losses from heat-related mortality allow city officials to allocate budgets efficiently focusing on areas where the benefits of such measures would be most effective.

Furthermore, this information could assist in strengthening medical services in areas with a high risk of HRM, particularly for vulnerable populations such as older adults aged 60 or over and those with chronic conditions, especially cardiovascular issues. Such a targeted approach could help reduce the impact of HRM on these groups and improve their overall health measures. In short, for effective administrative decisions regarding climate-related risks, it is crucial to create maps illustrating potential mortality and economic losses from HRM. This is particularly pertinent for large cities with populations exceeding one million. By adopting this approach, city planners can proactively address the growing challenges posed by climate change, safeguarding population health and enhancing a city's resilience.

Conclusions:

1. The methodology for mapping risks of ambient air overheating, premature mortality and economic losses has been created based on combining satellite remote sensing technology, epidemiological data and mathematical modeling. This methodology can serve as an informational support tool within a decision-making framework aimed at mitigating potential harm to population health in major cities due to climate change-related impacts.

2. The results of the satellite mapping, based on the case studies of Omsk and Rostov-on-Don, indicate deviations of up to 20 % in the estimated annual numbers of deaths and economic losses attributable to premature heat-related mortality. These levels of errors are within the acceptable range for urban planning and management decisions related to protecting public health in the context of climate change.

3. The distribution of potential specific HRM and economic losses demonstrates a non-uniform pattern within the city. Higher figures are concentrated in areas with a higher population density, while areas with lower population densities, such as industrial zones, green spaces or recreational zones experience minimal impact. Focusing on areas with high population densities constitutes a viable strategy for addressing public health concerns related to climate change.

4. The growing significance of geospatial data for the economy, society, and environment is determined by its role as information support of decision-making processes that de-

pend on spatially distributed economic information. This is a promising direction for the satellite remote sensing technology.

Funding. The research was carried out within:

- the budget theme of the Ministry of Science and Education of the Russian Federation: "SCIENTIFIC BASES FOR ASSESSING THE HEALTH OF ECO-SYSTEMS OF THE NORTH-WEST OF RUSSIA AND PREVENTION OF THREATS TO ENVIRONMENTAL SAFETY". Code FFZF-2022-0011;
- the implementation of the North-West Public Health Research Center research plan for 2021–2025, taking into account the national plan of measures for the second stage of adaptation to climate change up to 2025.

Competing interests. The authors declare no competing interests.

References

1. Allen M.R., Dube O.P., Solecki W., Aragón–Durand F., Cramer W., Humphreys S., Kainuma M., Kala J. [et al.]. Global warming of 1.5 °C: Special Report. *IPCC*, 2018, 616 p.

2. Koppe C., Kovats S., Jendritzky G., Menne B. Heat-waves: risks and responses. Copenhagen, WHO Regional Office for Europe, 2004, 123 p.

3. Shu C., Gaur A., Wang L., Lacasse M.A. Evolution of the local climate in Montreal and Ottawa before, during and after a heatwave and the effects on urban heat islands. *Sci. Total Environ.*, 2023, vol. 890, pp. 164497.

4. Ruuhela R., Jylha K., Lanki T., Tiittanen P., Matzarakis A. Biometeorological Assessment of Mortality Related to Extreme Temperatures in Helsinki Region, Finland 1972–2014. *Intern. J. Environ. Res. Public Health*, 2017, vol. 14, no. 8, pp. 944. DOI: 10.3390/ijerph14080944

5. Shartova N.V., Shaposhnikov D.A., Konstantinov P.I., Revich B.A. Air temperature and mortality: heat thresholds and population vulnerability study in Rostov-on-Don. *Fundamental'naya i prikladnaya klimatologiya*, 2019, no. 2, pp. 66–94. DOI: 10.21513/2410-8758-2019-2-66-94 (in Russian).

6. Vinogradova V.V., Zolotokrylin A.N. Current and Future Role of Climatic Factor in the Estimation of Natural Conditions of Life in Russia. *Izvestiya Rossiiskoi Akademii Nauk. Seriya Geograficheskaya*, 2014, no. 4, pp. 16–21. DOI: 10.15356/0373-2444-2014-4-16-21 (in Russian).

7. Andrade C. Understanding relative risk, odds ratio, and related terms: as simple as it can get. *J. Clin. Psychiatry*, 2015, vol. 76, no. 7, pp. e857-e861. DOI: 10.4088/JCP.15f10150

8. Guo Y., Gasparrini A., Li S., Sera F., Vicedo-Cabrera A.M., de Sousa Zanotti Stagliorio Coelho M., Nascimento Saldiva P.H., Lavigne E. [et al.]. Quantifying excess deaths related to heatwaves under climate change scenarios: A multicountry time series modelling study. *PLoS Med.*, 2018, vol. 15, no. 7, pp. e1002629. DOI: 10.1371/journal.pmed.1002629

9. Hanzlíková H., Plavcová E., Kynčl J., Kříž B., Kyselý J. Contrasting patterns of hot spell effects on morbidity and mortality for cardiovascular diseases in the Czech Republic, 1994–2009. *Int. J. Biometeorol.*, 2015, vol. 59, no. 11, pp. 1673–1684. DOI: 10.1007/s00484-015-0974-1

10. Urban A., Davídkovova H., Kysely J. Heat- and cold-stress effects on cardiovascular mortality and morbidity among urban and rural populations in the Czech Republic. *Int. J. Biometeorol.*, 2014, vol. 58, no. 6, pp. 1057–1068. DOI: 10.1007/s00484-013-0693-4

11. Salam A., Kamran S., Bibi R., Korashy H.M., Parray A., Mannai A.A., Ansari A.A., Kanikicharla K.K. [et al.]. Meteorological Factors and Seasonal Stroke Rates: A Four-year Comprehensive Study. *J. Stroke Cerebrovasc. Dis.*, 2019, vol. 28, no. 8, pp. 2324–2331. DOI: 10.1016/j.jstrokecerebrovasdis.2019.05.032

12. Zhao Q., Guo Y., Ye T., Gasparrini A., Tong S., Overcenco A., Urban A., Schneider A. [et al.]. Global, regional, and national burden of mortality associated with non-optimal ambient temperatures from 2000 to 2019: a three-stage modelling study. *Lancet Planet. Health*, 2021, vol. 5, no. 7, pp. e415–e425. DOI: 10.1016/S2542-5196(21)00081-4

13. Revich B.A., Grigorieva E.A. Health Risks to the Russian Population from Weather Extremes in the Beginning of the XXI Century. Part 1. Heat and Cold Waves. *Problemy analiza riska*, 2021, vol. 18, no. 2, pp. 12–33. DOI: 10.32686/1812-5220-2021-18-2-12-33 (in Russian).

14. Kritsuk S.G., Gornyy V.I., Latypov I.Sh., Pavlovskii A.A., Tronin A.A. Satellite Risk Mapping of Urban Surface Overheating (by the Example of Saint Petersburg). *Sovremennye problemy distantsionnogo zondirovaniya Zemli iz kosmosa*, 2019, vol. 16, no. 5, pp. 34–44. DOI: 10.21046/2070-7401-2019-16-5-34-44 (in Russian).

15. Kritsuk S., Gornyy V., Davidan T., Latypov I., Manvelova A., Konstantinov P., Tronin A., Varentsov M., Vasiliev M. Satellite mapping of air temperature under polar night conditions. *Geo-spatial Information Science*, 2022, vol. 25, no. 2, pp. 325–336. DOI: 10.1080/10095020.2021.2003166

16. Gornyy V.I., Kritsuk S.G., Latypov I.Sh., Manvelova A.B., Tronin A.A. Satellite Mapping of Urban Air Overheating Risk (Case Study of Helsinki, Finland). *Cosmic Res*., 2022, no. 60, suppl. 1, pp. S38–S45. DOI: 10.1134/S0010952522700058

17. Gornyy V.I., Kritsuk S.G., Latypov I.Sh., Tronin A.A. Satellite Mapping of Economic Damage from Urban Deaths Caused by Overheating (by Example of Helsinki, Finland). *Sovremennye problemy distantsionnogo zondirovaniya Zemli iz kosmosa*, 2022, vol. 19, no. 3, pp. 35–46. DOI: 10.21046/2070-7401-2022-19-3-35-46 (in Russian).

18. Srivanit M., Hokao K. Thermal Infrared Remote Sensing for Urban Climate and Environmental Studies: An Application for the City of Bangkok, Thailand. *JARS*, 2012, vol. 9, no. 1, pp. 83–100. DOI: 10.56261/jars.v9i1.168598

19. Smargiassi A., Goldberg M.S., Plante C., Fournier M., Baudouin Y., Kosatsky T. Variation of daily warm season mortality as a function of micro-urban heat islands. *J. Epidemiol. Community Health*, 2009, vol. 63, no. 8, pp. 659–664. DOI: 10.1136/jech.2008.078147

20. Ho H.C., Knudby A., Huang W. Spatial Framework to Map Heat Health Risks at Multiple Scales. *Int. J. Environ. Res. Public Health*, 2015, vol. 12, no. 12, pp. 16110–16123. DOI: 10.3390/ijerph121215046

21. Ho H.C., Knudby A., Xu Y., Hodul M., Aminipouri M. A comparison of urban heat islands mapped using skin temperature, air temperature, and apparent temperature (Humidex), for the greater Vancouver area. *Sci. Total Environ.*, 2016, vol. 544, pp. 929–938. DOI: 10.1016/j.scitotenv.2015.12.021

22. Ho H.C., Knudby A., Walker B.B., Henderson S.B. Delineation of Spatial Variability in the Temperature-Mortality Relationship on Extremely Hot Days in Greater Vancouver, Canada. *Environ. Health Perspect.*, 2017, vol. 125, no. 1, pp. 66–75. DOI: 10.1289/EHP224

23. Zubets A.N., Novikov A.V. Quantitative assessment of the value of human life in Russia and in the world. *Finance: Theory and Practice*, 2018, vol. 22, no. 4, pp. 52–75. DOI: 10.26794/2587-5671-2018-22-4-52-75 (in Russian).

24. Barsi J.A., Schott J.R., Palluconi F.D., Helder D.L., Hook S.J., Markham B.L., Chander G., O'Donnell E.M. Landsat TM and ETM+ thermal band calibration. *Can. J. Remote Sensing*, 2003, vol. 29, no. 2, pp. 141–153. DOI: 10.5589/m02-087

25. Dominguez-Delgado A., Domínguez-Torres H., Domínguez-Torres C.-A. Energy and Economic Life Cycle Assessment of Cool Roofs Applied to the Refurbishment of Social Housing in Southern Spain. *Sustainability*, 2020, vol. 12, no. 14, pp. 5602. DOI: 10.3390/su12145602

Gornyy V.I., Kritsuk S.G., Latypov I.Sh., Tronin A.A., Buzinov R.V., Noskov S.N., Yeremin G.B., Borisova D.S. Assessing economic losses from risks of heat-related premature mortality using satellite mapping in Russian megacities. Health Risk Analysis, 2025, no. 2, pp. 46–59. DOI: 10.21668/health.risk/2025.2.04.eng

Received: 23.05.2025
Approved: 09.06.2025
Accepted for publication: 26.06.2025